

Trap loss in a two-species Na-Cs magneto-optical trap: Intramultiplet mixing in heteronuclear ultracold collisions

James P. Shaffer,* Witek Chalupczak, and N. P. Bigelow

*Department of Physics and Astronomy and The Laboratory for Laser Energetics,
The University of Rochester, Rochester, New York 14627*

(Received 12 April 1999)

We describe a comprehensive investigation of trap loss in a two-species Na-Cs magneto-optical trap. Observed losses, due to the interspecies interactions, are attributed to collisions in which a change in the fine-structure state of the Na partner causes the escape of atoms from the trap. Results are described in terms of the heteronuclear pair potentials and the interaction of the colliding pairs with the radiatively active environment. [S1050-2947(99)51710-1]

PACS number(s): 32.80.Pj, 34.50.Rk

In recent years there has been significant interest in the physics of ultracold collisions of laser-cooled and trapped atoms [1]. More recently, a new interest has developed concerning the physics of ultracold vapors composed of more than one atomic species [2].

In the homonuclear alkali-metal-atom magneto-optical trap (MOT) we consider two types of excited-state ultracold collisions [3]. Both begin when two ground-state atoms absorb a trapping laser photon at an internuclear separation of ~ 800 Å. The ground-ground-state pair potential V_{gg} (dipole-dipole $\sim 1/R^6$) and the ground-excited-state pair potential V_{ge} (attractive resonant-dipole $\sim 1/R^3$) bring the colliding pair into resonance with the trapping fields, a photon is absorbed, and a molecule is created by photoassociation. As the nuclei slowly accelerate towards one another the complex may radiate, transferring kinetic energy $\Delta\epsilon_{RE}$ to the pair. If $\Delta\epsilon_{RE}$ is greater than the trap depth the atoms will escape. This process is called radiative escape (RE). The second type of process occurs when the photoassociated complex undergoes intramultiplet mixing resulting in a change in fine-structure (FS) state. In general, $\Delta\epsilon_{FS}$ far exceeds the MOT depth and all FS collisions result in loss. The reaction is induced at long range by the resonant dipole interaction, or at close range in the region of exchange-type interactions. Close-range couplings may be via heterogeneous interactions (Coriolis effects), or by spin-orbit (SO) mixing [4,5].

The heteronuclear case is different because there is no long-range resonant dipole contribution to V_{ge} . One consequence is that the pair comes into resonance with the trap lasers at much smaller internuclear spacing than for the homonuclear case. The result is twofold: first, the probability of RE is drastically reduced [6]; and second, changes of FS all occur at short range (< 20 Å). Heteronuclear trap-loss collisions, then, are dominated by close-range photoassociation (PA) events resulting in intermultiplet mixing (IM) and either FS change or excitation exchange (EE : $A + B^* \rightarrow A^* + B$).

As a result of symmetry and energy considerations there are six possible IM processes in a heteronuclear alkali-metal system (see Fig. 1). Because the trapping transition is $n^2S_{1/2} \rightarrow n^2P_{3/2}$, the system is dilute ($\rho \sim 10^{10} \text{ cm}^{-3}$) and $T < 1$ mK [initial kinetic energy ($E_{int,k}$) $\ll \Delta\epsilon_{FS}$], only three of the six possible processes can be observed in our MOT:

$$\text{Na}(P_{3/2}) + \text{Cs}(S_{1/2}) \rightarrow \text{Na}(P_{1/2}) + \text{Cs}(S_{1/2}) + \Delta\epsilon_{\text{NaFS}},$$

$$\text{Na}(P_{3/2}) + \text{Cs}(S_{1/2}) \rightarrow \text{Na}(S_{1/2}) + \text{Cs}(P_{3/2}) + \Delta\epsilon_{\text{EE}},$$

$$\text{Na}(S_{1/2}) + \text{Cs}(P_{3/2}) \rightarrow \text{Na}(S_{1/2}) + \text{Cs}(P_{1/2}) + \Delta\epsilon_{\text{CsFS}}.$$

Here $\Delta\epsilon_{\text{NaFS}} = 17 \text{ cm}^{-1}$, $\Delta\epsilon_{\text{EE}} = 5241 \text{ cm}^{-1}$, and $\Delta\epsilon_{\text{CsFS}} = 554 \text{ cm}^{-1}$. We refer to these as Na+Cs:NaFS, Na+Cs:EE, and Na+Cs:CsFS, respectively. In this paper we focus on the roles of each of these processes in our Na+Cs MOT (2MOT).

Trapping laser beams contain light at $\lambda_{\text{Na}} = 589 \text{ nm}$ and $\lambda_{\text{Cs}} = 852 \text{ nm}$ (frequency stability < 1 MHz) tuned by reference to saturated absorption spectrometers. The Na trap laser is detuned by $\Delta_{\text{Na}} = -13 \text{ MHz}$ from the $3^2S_{1/2}(F=2)$

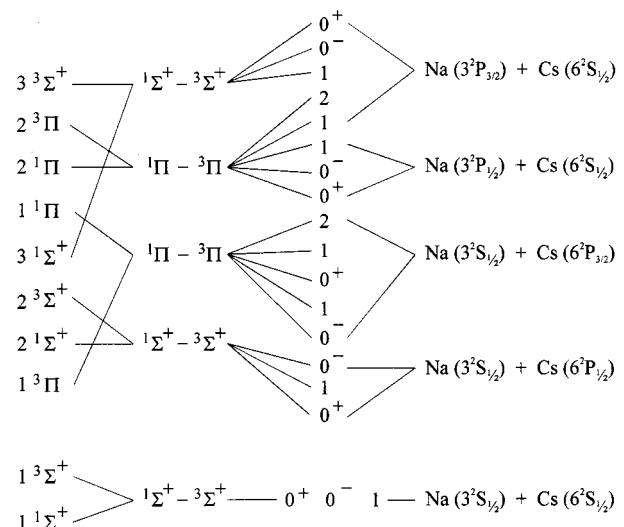


FIG. 1. Correlation diagram for NaCs. The diagram includes the D1 and D2 multiplets and combinations for Na and Cs.

*Present address: The Institute of Optics, The University of Rochester.

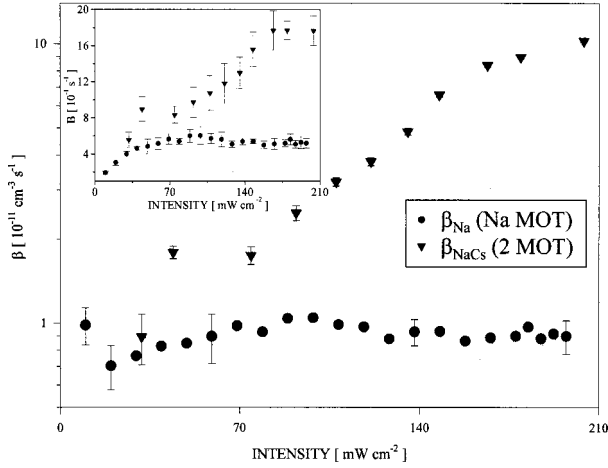


FIG. 2. $\beta_{\text{Na}}(I_{\text{Na}})$ and $\beta_{\text{NaCs}}(I_{\text{Na}}, I_{\text{Cs}} = 230 \text{ mW/cm}^2)$ as a function of I_{Na} for Na loss. Each I_{Na} is the total six-beam trap laser intensity. The inset shows the absolute trap loss rates $\equiv B_{\text{Na}}(I_{\text{Na}})$ and $B_{\text{NaCs}}(I_{\text{Na}}, I_{\text{Cs}} = 230 \text{ mW/cm}^2)$ for Na.

$\rightarrow 3^2P_{3/2}(F'=3) D2$ transition. The 589-nm light is passed through an electro-optic modulator that introduces sidebands shifted from the input by ± 1.71 GHz. The blue detuned sideband couples the $F=1$ to $F'=2$ transition, preventing loss due to optical pumping. The intensity of each sideband is 10% of the total intensity. The 852-nm light is detuned $\Delta_{\text{Cs}} = -23$ MHz from the $6^2S_{1/2}(F=4) \rightarrow 6^2P_{3/2}(F'=5)$ $D2$ transition. Cs repumping light is provided by a stabilized diode laser tuned to the $F=3 \rightarrow F'=4$ transition (intensity 1.5 mW/cm^2). Anti-Helmholtz coils produce a field gradient of 20 G/cm . The traps are loaded using uncooled sources at 10^{-10} Torr.

We determine the number of atoms from the fluorescence of each trapped species using narrow-band ($\Delta\lambda = 9 \text{ nm}$) interference filters and calibrated photomultiplier tubes (PMT's). Trap sizes and shapes were measured with interference filters and two calibrated charge-coupled-device (CCD) cameras (resolution $< 30 \mu\text{m}$) oriented so that complete three dimensional overlap of the Cs and Na clouds could be assured. The number of atoms was obtained from the fluorescence rate using a steady-state two-field six-level calculation. Individual trapped atom densities were $\sim 10^{10} \text{ cm}^{-3}$ with $\sim 10^6$ Na atoms and $\sim 10^7$ Cs atoms. Under these conditions multiple-scattering effects are negligible [7].

The collision rates in the 2MOT were initially examined by analysis of the trap loading. We describe the loading rate of species i in the presence of species j as, $dN_i(t)/dt = L - \alpha_i N_i(t) - \beta_{ij} N_j(t) N_i(t) / V - \beta_i N_i^2(t) / V$, where β_{ij} is the loss rate from ultracold collisions between species i and species j , N is the number atoms, L is the trap loading rate, β_i is the single species ultracold collision loss rate, α_i is the loss rate due to background collisions, and V is the trap volume. This rate equation is a Riccati equation, which we solve explicitly [8]. A series of trap filling experiments were carried out to determine the $\beta_{\text{Na}}(I_{\text{Na}})$, $\beta_{\text{Cs}}(I_{\text{Cs}})$ and $\beta_{\text{NaCs}}(I_{\text{Na}}, I_{\text{Cs}})$.

First we measured $N_{\text{Na}}(t)$ for the Na trap with and without Cs in the trap. Figure 2 shows the trap loss rates $\beta_{\text{Na}}(I_{\text{Na}})$ for the pure Na MOT and $\beta_{\text{NaCs}}(I_{\text{Na}}, I_{\text{Cs}} = 230 \text{ mW/cm}^2)$ for the 2MOT. $\beta_{\text{Na}}(I_{\text{Na}})$ agrees well with published values [9]. There are two striking results: (i) $\beta_{\text{NaCs}}(I_{\text{Na}}, I_{\text{Cs}}$

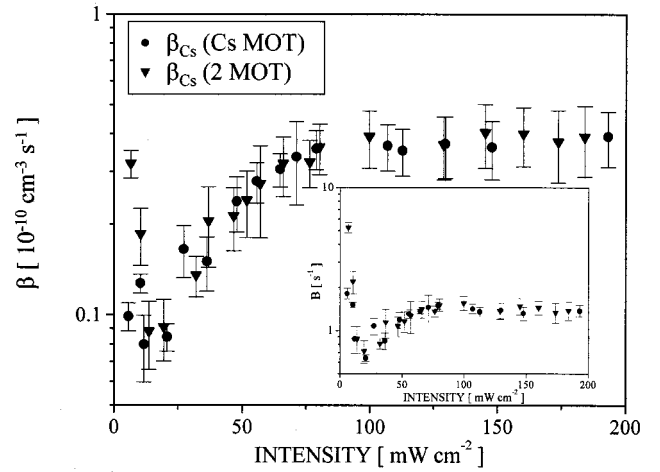


FIG. 3. Cs cold collision loss rate $\beta_{\text{Cs}}(I_{\text{Cs}})$ as a function of I_{Cs} for loss from the Cs trap and for the Na+Cs trap. For the 2MOT data, $I_{\text{Na}} = 88 \text{ mW/cm}^2$. Here, we extract β_{Cs} for the 2MOT by neglecting β_{NaCs} (see text). I_{Cs} is the total six-beam trap laser intensity. The inset shows the absolute trap loss rates $\equiv B_{\text{Cs}}(I_{\text{Cs}})$ and $B_{\text{NaCs}}(I_{\text{Na}} = 88 \text{ mW/cm}^2, I_{\text{Cs}})$ for Cs.

$= 230 \text{ mW/cm}^2$) can be almost an order of magnitude greater than $\beta_{\text{Na}}(I_{\text{Na}})$ and (ii) during the Na filling measurement made with Cs atoms in the trap, the Cs atom number and density remain essentially constant. Since these measurements took place with the same Cs and Na background pressures, we exclude collisions between background Cs atoms and trapped Na atoms as the reason for additional Na loss in the 2MOT. By comparing the intensity dependence of β_{Na} and β_{NaCs} we conclude that the two-species loss is not due to Na hyperfine changing collisions. Specifically, β_{NaCs} continues to increase for $I_{\text{Na}} > 35 \text{ mW/cm}^2$, where the capture energy (the ‘‘trap depth’’) of the MOT has far exceeded the Na hyperfine-splitting energy [9,10].

In the next set of experiments we examine the filling of Cs atoms in the trap with and without Na atoms present. To illustrate the weak effect of the Na on the trapped Cs, we first extract β_{Cs} , neglecting the effects of β_{NaCs} [11]. Figure 3 shows the resulting $\beta_{\text{Cs}}(I_{\text{Cs}})$ for a pure Cs trap and for the 2MOT ($I_{\text{Na}} = 88 \text{ mW/cm}^2$). We note that $\beta_{\text{Cs}}(I_{\text{Cs}})$ agrees with published values [12]. In both measurements, β_{Cs} does not noticeably change with I_{Cs} for $I_{\text{Cs}} > 80 \text{ mW/cm}^2$.

To explore the two-species losses further, we made Cs filling measurements as a function of I_{Na} fitting the data including both β_{Cs} and β_{NaCs} . In Fig. 4 we show results for $\beta_{\text{NaCs}}(I_{\text{Na}}, I_{\text{Cs}} = 221 \text{ mW/cm}^2)$. Here I_{Cs} was specifically chosen because at this intensity $\beta_{\text{Cs}}(I_{\text{Cs}})$ is approximately independent of I_{Cs} . Similar results were obtained for other values of I_{Cs} . Considering β_{NaCs} as measured from both Cs and Na filling experiments, we find that for $75 < I_{\text{Na}} < 180 \text{ mW/cm}^2$ $\beta_{\text{NaCs}}(I_{\text{Na}})$ is best fit by a first-order polynomial in I_{Na} . The slopes $\partial\beta_{\text{NaCs}}/\partial I_{\text{Na}}$ from these fits agree to within 10%, which was comparable to the reliability in the individual fits. We therefore conclude that the dominant two-species losses involve one excited Na atom [5,13] and consequently the absorption of one 589 nm photon. Furthermore, because $\beta_{\text{NaCs}}(I_{\text{Na}}, I_{\text{Cs}})$ does not change with I_{Cs} , we conclude that these collisions involve one ground-state Cs atom. Finally, since (i) the β_{NaCs} measured from Cs trap

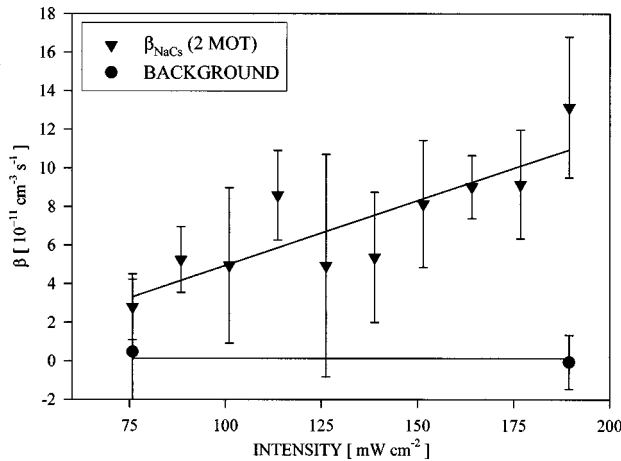


FIG. 4. $\beta_{\text{NaCs}}(I_{\text{Na}}, 221 \text{ mW/cm}^2)$ for a measurement of Cs trap loss. The baseline (circles) represent the background fluctuations of the Cs trap in absence of trapped Na.

loading agrees with the β_{NaCs} measured from Na trap loading and (ii) we observe β_{NaCs} to change with I_{Na} for $I_{\text{Cs}} = 221 \text{ mW/cm}^2$, we conclude that the two-species loss is not due to Cs hyperfine changing collisions.

Given that the Cs atom is in its ground state, Na +Cs:CsFS cannot be important (it requires an excited Cs atom). We nevertheless attempted to directly detect Na +Cs:CsFS by measuring the Cs FS rate in the 2MOT and comparing it with that of a pure Cs MOT. Measurement of the Cs FS rate was made by detecting D1 fluorescence through a 10-nm bandwidth filter followed by a SPEX 1700-2 1-m monochromator with $< 8 \text{ \AA}$ bandpass. Photons passing through the system were detected by an avalanche photodiode (dark counts $\sim 50 \text{ Hz}$). We measured the FS rate for pure Cs trap as a function of I_{Cs} from 5 mW/cm^2 to 300 mW/cm^2 [10] and found no modification of the Cs FS rate when the Na MOT was present. The resolution was 6 s^{-1} , placing an upper bound for $\beta_{\text{Na+Cs:CsFS}}$ of $5 \times 10^{-13} \text{ cm}^3 \text{ s}^{-1}$, thus ruling out Na+Cs:CsFS as a key contributor to loss in the 2MOT.

Na+Cs:EE has not yet been ruled out, so we attempted to observe it directly. We extinguished the Cs trap light for $50 \mu\text{s}$ and during this period, we searched for the production of Cs D2 photons. We saw no signal due to Na+Cs:EE. The resolution was 20 s^{-1} with a background count rate of 100 Hz . This places an upper bound $\beta_{\text{Na+Cs:EE}} < 3 \times 10^{-13} \text{ cm}^3 \text{ s}^{-1}$, meaning that Na+Cs:EE makes a negligible contribution to β_{NaCs} .

Having ruled out Na+Cs:CsFS and Na+Cs:EE, we conclude [14] that $\beta_{\text{NaCs}}(I_{\text{Na}}, I_{\text{Cs}})$ is dominated by Na +Cs:NaFS. The fact that Na+Cs:NaFS should dominate the possible intramultiplet mixing processes is consistent with the scaling of the energy defects $\Delta \epsilon_{\text{NaFS}} = 17 \text{ cm}^{-1}$, $\Delta \epsilon_{\text{EE}} = 5241 \text{ cm}^{-1}$, and $\Delta \epsilon_{\text{CsFS}} = 554 \text{ cm}^{-1}$.

Calculations [15,16] show that all the long-range Hund's case (c) potentials in the NaCs* manifold are attractive. In the Na*Cs manifold, the case (c) states $0^+, 0^-, 1$ correlating with Cs($6^2S_{1/2}$) + Na($3^2P_{1/2}$) and $0^-, 1, 2$ correlating with Cs($6^2S_{1/2}$) + Na($3^2P_{3/2}$) are attractive. An important point is that for NaCs the Hund's case (c) states correlating to the Cs($6^2S_{1/2}$) + Na($3^2P_{1/2}$) asymptote are *all attractive* and so

there is no effective shielding by any long-range repulsive states correlating to this asymptote.

Heteronuclear intermultiplet mixing occurs with the same type of close-range mechanisms as the homonuclear case (SO and Coriolis mixing) [17]. Consideration of the correlation diagram (Fig. 1) allows us to exclude some pathways. The channel leading to SO change at the $3^1\Sigma^+ - 2^3\Pi$ or $3^1\Sigma^+ - 2^1\Pi$ crossing is closed because the 0^+ state is repulsive at long range and there is no first-order mixing between 0^- and 0^+ [18]. This leaves only two channels for Na+Cs:NaFS: SO merging of the $2^1\Pi_1$ and $2^3\Pi(^3\Pi_1)$ states and Coriolis mixing of the $2^3\Pi$ state. Similar inspection of Fig. 1 explains why Na+Cs:CsFS should be weak: there is neither strong Coriolis mixing nor SO merging between the two states, which could lead to a FS change: the $1^1\Pi_1$ and $3^1\Pi_1$ states. The lower asymptote does admit SO coupling of $2^1\Sigma^+ - 1^3\Pi$ and $2^1\Sigma^+ - 1^3\Pi$, but these will be shown to be small.

Since the reduced mass of NaCs is only 19.6 amu we expect Coriolis coupling to dominate the Na+Cs:NaFS cross section, just as in the Na+Na case [4,5]. Coriolis-induced NaFS occurs as Hund's case (a) breaks down becoming case (b) coupling (S uncoupling). The same process occurs when an excited alkali-metal atom collides with a noble-gas atom [19]. This mechanism favors Na+Cs:NaFS, since the case(a) to case(b) uncoupling parameter is proportional to the SO splitting [20].

The second path, a merging of $2^1\Pi$ and the $2^3\Pi$ due to the SO interaction, occurs in the transition from Hund's case (c) coupling to case (a) coupling. This mechanism is also a result of a time-dependent field created as the electron spin decouples from the orbital angular momentum. This occurs when other interactions (mostly exchange) become comparable to the atomic SO interaction and there is a resulting breakdown of case (c) coupling [19]. The only nonzero matrix element, to first order, is $\langle 2^1\Pi_1 | H_{\text{SO}} | 2^3\Pi_1 \rangle$. The coupling between the $2^1\Pi$ and the $2^3\Pi$ states has been estimated [17] to be $\Delta \epsilon_{\text{CsFS}} - \Delta \epsilon_{\text{NaFS}} / 6$. The fact that $\Delta \epsilon_{\text{NaFS}} < \langle 2^1\Pi_1 | H_{\text{SO}} | 2^3\Pi_1 \rangle$ indicates that, although we believe that the SO mechanism is of less importance than the Coriolis, the SO cannot be automatically dismissed. We note that in general for heteronuclear collisions this channel becomes increasingly important as the mass of the molecule increases.

The Na+Cs:CsFS rate is small because the SO coupling between $2^1\Sigma^+ - 1^3\Pi$ and $2^1\Sigma^+ - 1^3\Pi$ is less than the Cs SO splitting. The largest SO coupling between the $2^1\Sigma^+$ and $1^3\Pi_{0^+}$ states has been found [17] to be $\sqrt{2}(\Delta \epsilon_{\text{NaFS}} + \Delta \epsilon_{\text{CsFS}}) / 6$ and the $3^1\Sigma^+$ and $3^1\Pi_1$ states to be $(\Delta \epsilon_{\text{NaFS}} + \Delta \epsilon_{\text{CsFS}}) / 6$. In both cases we find the interaction energy to be less than the FS splitting in the NaCs* manifold.

The cross section for EE has been evaluated [17] and is small — since $\Delta \epsilon_{\text{EE}}$ is large, this probability is negligible. Experiments on K+Rb collisions at 370 K give cross sections for EE of $\sim 2\text{-}40 \text{ \AA}^2$ [17]. The cross sections for Na +Cs:EE can be expected to be much smaller since $\Delta \epsilon_{\text{EE}}(\text{KRb}) / \Delta \epsilon_{\text{EE}}(\text{NaCs}) = 0.043$. This is consistent with our work: EE in Na+Cs appears to be absent.

The loss rate we infer as due to Na+Cs:NaFS is large compared to both measured and predicted FS rates for homonuclear collisions. This is not surprising because heteronuclear molecules with weak (C_6/R^6) van der Waals poten-

tials on the $S+P$ asymptotes have more favorable $g+g$ to $g+e$ Franck-Condon factors than homonuclear molecules that have strong attractive resonant dipole-dipole interactions (C_3/R^3) [15]. The fact that the collision begins at smaller internuclear spacings than the homonuclear counterpart also means that the heteronuclear attempt rate for the reaction is larger: in the homonuclear system the time scale for the collision allows only a single passage through the transition region, whereas in the heteronuclear case the photoassociated quasimolecule has time to vibrate several times before it decays (most likely at the outer turning point where the Franck-Condon factors are large) or dissociates.

In conclusion, we have presented an extensive study of a heteronuclear ultracold trap-loss inducing reactive collision. We have obtained estimates for cross sections of various

intramultiplet mixing processes for Na+Cs. Our differential measurements have been able to discriminate the input channels and states contributing to the Na+Cs:NaFS process. We have concluded that the significant mechanisms that lead to Na+Cs:NaFs are Coriolis mixing of $2^3\Pi_{1,2}$ with the $2^3\Pi_{0\pm}$ levels and SO merging of $2^3\Pi_1$ with $2^1\Pi_1$. This measurement provides experimental information to motivate calculations that may help to provide a full understanding of both homonuclear and heteronuclear ultracold collisions.

We thank P. Julienne and C. Williams for important discussions. This work was supported by the National Science Foundation and the David and Lucille Packard Foundation. J.P.S. thanks the Horton Foundation.

-
- [1] H. Wang *et al.*, *Z. Phys. D* **36**, 317 (1996); P. D. Lett *et al.*, *Annu. Rev. Phys. Chem.* **46**, 423 (1995), and references therein.
- [2] M. Santos *et al.*, *Phys. Rev. A* **52**, R4340 (1995); J. P. Shaffer *et al.*, *Phys. Rev. Lett.* **82**, 1124 (1999); G. D. Telles *et al.*, *Phys. Rev. A* **59**, R23 (1999); W. Suptitz *et al.*, *Opt. Lett.* **19**, 1571 (1994).
- [3] J. Weiner, *Adv. At., Mol., Opt. Phys.* **35**, 45 (1995); J. Weiner *et al.*, *Rev. Mod. Phys.* **71**, 1 (1999), and references therein.
- [4] E. I. Dashevskaya, *Opt. Spektrosk.* **46**, 423 (1979) [*Opt. Spectrosc.* **46**, 236 (1979)]; E. I. Dashevskaya *et al.*, *Can. J. Phys.* **47**, 1237 (1969).
- [5] P. S. Julienne and J. Vigue, *Phys. Rev. A* **44**, 4464 (1991).
- [6] Γ , the excited-state lifetime, should not change significantly while the interatomic separation where the initial excitation takes place is one order of magnitude smaller.
- [7] D. W. Sesko *et al.*, *J. Opt. Soc. Am. B* **8**, 946 (1991); T. G. Walker *et al.*, *Phys. Rev. Lett.* **64**, 408 (1990).
- [8] J. P. Shaffer *et al.*, *App. Phys. B* (to be published).
- [9] S-Q. Shang *et al.*, *Phys. Rev. A* **50**, R4449 (1994); L. Marcassa *et al.*, *ibid.* **47**, R4563 (1988).
- [10] J. P. Shaffer *et al.*, *Eur. Phys. J. D* (to be published).
- [11] Note that over a large range of I_{Cs} values $\beta_{NaCs}(88 \text{ mW/cm}^2, I_{Cs}) N_{Na} \ll \beta_{Cs}(I_{Cs}) N_{Cs}$, such that the loss rate of Cs atoms due to Cs-Cs collisions is much larger than that due to Na-Cs collisions.
- [12] D. Sesko *et al.*, *Phys. Rev. Lett.* **63**, 961 (1989).
- [13] A. Gallagher and D. E. Pritchard, *Phys. Rev. Lett.* **63**, 957 (1989).
- [14] Ideally, it would have been better to measure process (i) directly but the 6-Å separation of the Na D1 and D2 lines and rate of FS changing collisions make such a measurement extremely difficult. We also attempted to measure this rate by multiphoton ionization of the collision fragments, but the signal was obscured by the molecular structure near the atomic resonances.
- [15] W. C. Stwalley and H. Wang, *J. Chem. Phys.* **108**, 5767 (1998).
- [16] M. Movre and R. Beuc, *Phys. Rev. A* **31**, 2957 (1985); B. Bussery *et al.*, *Chem. Phys.* **116**, 319 (1987).
- [17] E. I. Dashevskaya *et al.*, *Can. J. Phys.* **48**, 981 (1970); E. E. Nikitan, *Adv. Chem. Phys.* **28**, 317 (1975), and references therein.
- [18] I. Kovacs, *Can. J. Phys.* **36**, 309 (1958).
- [19] E. I. Dashevskaya *et al.*, *J. Chem. Phys.* **55**, 1175 (1970). Here a time-dependent magnetic field associated with rotation of the collision axis induces an electronic spin flip
- [20] G. Herzberg, *Molecular Spectra and Molecular Spectra of Diatomic Molecules* (Krieger Publishing, Malabar, FL, 1989).